Proceedings of the ASME 2013 International Mechanical Engineering Congress & Exposition
IMECE 2013
November 13-21, 2013, San Diego, California, USA

Final Paper IMECE 2013-66419

3D Packaging Materials based on Graphite Nanoplatelet and Aluminum Nitride Nanocomposites

Srilakshmi Lingamneni
Department of Mechanical Engineering
Stanford University
Stanford, CA, USA
sril@stanford.edu

Amy M. Marconnet
Department of Mechanical Engineering
Massachusetts Institue of technology
Cambridge, MA , USA
amymarco@mit.edu

Kenneth E. Goodson
Department of Mechanical Engineering
Stanford University
Stanford, CA, USA
goodson@stanford.edu

ABSTRACT:

Nanostructured composites with efficient percolation networks are promising candidates for packaging materials due to their high thermal conductivity. In this study, we investigate the thermal conductivity of composites consisting of a combination of exfoliated graphene nanoplatelet (xGNP) and aluminum nitride (AlN) particles in polyvinylidine fluoride (PVDF) matrix. The surfaces of the AlN particles are treated with silane to reduce the interfacial thermal resistance at particle-matrix boundary. Samples with 50 vol% AlN and 2 vol% xGNP showed an order of magnitude enhancement in thermal conductivity. AlN composites (with and with out xGNP) showed evidence of effective percolation pathways for AlN vol % over ~40.

KEY WORDS: Nanocomposites, exfoliated graphene, aluminum nitride, thermal conductivity, percolation

NOMENCLATURE

k	Thermal conductivity
dT/dx	Temperature gradient
f	Volume fraction of filler particles
PVDF	Polyvinylidine fluoride
xGNP	Exfoliated graphene nanoplatelets
AlN	Aluminum nitride
SiC	Silicon carbide
MWCNT	Multi-wall carbon nano tubes
BN	Boron nitride
hBN	Hexagonal boron nitride
cBN	Cubic boron nitride
Ni	Nickel
Fe_3O_4	Magnetite
SiO_2	Silica
Al_2O_3	Alumina

Subscripts:

w	Whiskers
m	Matrix
e	Effective
p	Filler particle
ref	Reference (quartz)
sam	Sample
ref, cold	Reference on cold side
Ref, hot	Reference on hot side

1 INTRODUCTION

In recent years, there has been a shift from conventional 2D Integrated Circuits to 2.5D or 3D integration in order to improve device performance. However, this three dimensional circuit integration requires improvements in thermal management to address various reliability challenges including mechanical failure caused by thermal stresses, increased surface heat fluxes

and internal temperature rises[1, 2]. These challenges can be addressed by the development of novel interface and underfill materials with improved thermal conductivity [3]. These materials must maintain the required additional properties including adhesive strength, viscosity, elastic modulus, and electrical resistivity.

Filler particles such as aluminum nitride, silicon carbide, boron nitride, diamond, alumina and, silica have traditionally been used to synthesize composites that are electrically insulating but thermally conducting [8, 10, 11]. Very high volume fractions of these filler particles are needed to achieve at least an order of magnitude enhancement in thermal conductivity due to the moderate thermal conductivity and ~ 1 aspect ratio of the filler particles. On the other hand, thermal conductivity enhancement can be achieved very efficiently using thermally exfoliated graphene nanoplatelets [12, 13]. But, the high electrical conductivity of graphene substantially increases the electrical conductivity of the composites [14].

	Filler	Reference
■	Magnetite (Fe_3O_4)	Philip *et al.*[4]
▲	Nickel (Ni) and MWCNT	Hu *et al.*[5]
✱	Boron nitride (BN) and MWCNT	Teng *et al.*[6]
◆	BN with multi-modal particle size mixing	Yung *et al.*[7]
●	AlN whiskers and particles	Xu *et al.*[8]
+	Three dimensional AlN nanowhiskers	Shi *et al.*[9]
○	Silicon carbide (SiC)	Zhou *et al.*[10]
×	Alumina (Al_2O_3)	Fu *et al.*[11]
△	Silica (SiO_2)	Lee *et al.*[11]
◇	Diamond	Lee *et al.*[11]
□	Exfoliated graphene nanoplatelets (xGNP)	Yu *et al.*[13]

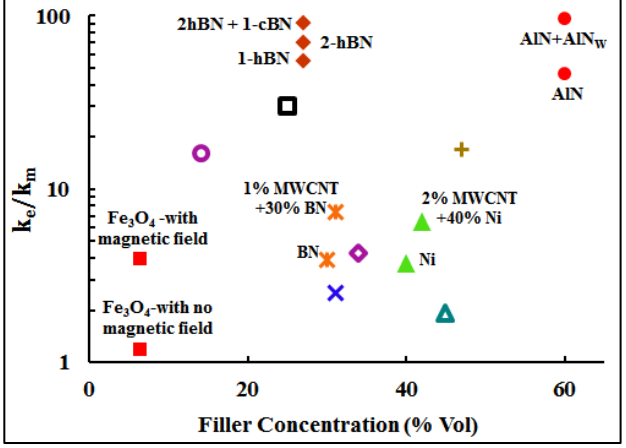

Figure 1. Past data for the thermal conductivity enhancement for various filler materials from literature as a function of total filler volume fraction. The chart lists the different filler particles used in the composites, a subset of which are indicated directly on the plot where efficient percolation pathways are established.

Figure 1 shows the thermal conductivity enhancement in composites made from a variety of materials. (Thermal conductivity enhancement is calculated as the ratio of thermal conductivity of the composite to that of the matrix material). The effective thermal conductivity of composites is often limited by the low thermal conductivity of matrix materials at low filler volume fractions. Beyond a threshold filler volume fraction, effective percolation pathways are established by the filler particles and the low thermal conductivity of the matrix is bypassed by the low resistance network established by the filler particles. This threshold filler volume fraction is high for ~1 aspect ratio particles, and is as low as a few vol% for high aspect ratio particles like carbon nano tubes (CNTs) and graphene.

Several methods have been adopted to establish efficient percolation networks in composites. Application of magnetic field on magnetic filler particles [4], use of a combination of high and low aspect ratio particles [5, 6], multi-modal particle size and shape mixing [7, 8] and use of three dimensional particles with nanowhiskers [9] are some methods that showed substantial enhancements in thermal conductivity. In addition, use of more than one filler material provides additional degrees of freedom to design composites that have desired mechanical, thermal and electrical properties.

In this work, we investigate the thermal conductivity of nanocomposites consisting of exfoliated graphite nanoplatelet and aluminum nitride inclusions in Polyvinylidene fluoride. While xGNPs have very high electrical and thermal conductivities, AlN particles are electrically insulating with moderate thermal conductivity. Silane treating the AlN particles facilitates stable bonding between the particles and PVDF. The thermal conductivity of the nanocomposites are characterized using infrared microscopy technique.

2 EXPERIEMNTAL METHODS

2.1 Materials

In this work, we fabricate composites consisting of xGNP particles (grade M, XG Sciences) and AlN particles (Sigma-Aldrich) embedded in a polyvinylidene fluoride matrix (Sigma-Aldrich). As shown in Figure 2, the xGNP particles are sheets with an average thickness of 6-8 nm and width of 5 µm and the AlN particles have a maximum size of 10 µm. The AlN particles are silane treated with (3-Aminopropyl)triethoxysilane (Sigma-Aldrich) to improve the bonding to the PVDF matrix.

2.2 Sample preparation

2.2.1 Silane treatment

First, to facilitate particle-matrix coupling, the AlN particles are treated with (3-Aminopropyl)-triethoxysilane (see Figure 3). Specifically, 2 mL of silane is added to each 100 mL of 5% aqueous solution of ethanol. Then, the AlN particles are added to the solution and stirred for

1 h while maintaining the temperature of the solution at 70°C. The particles are then rinsed with ethanol 3 times, separated from the solution using centrifuging, and dried in an oven at 110ºC for 18 h. During silane treatment, silane molecules attach to the AlN particles through hydrolysis of ethoxy groups, while the amine branch of the silane allows coupling with PVDF matrix. This coupling reduces thermal boundary resistance between the matrix and AlN particles [15].

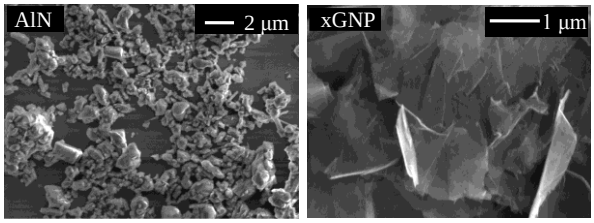

Figure 2. SEM imgaes of AlN and xGNP particles showing particle shapes and sizes.

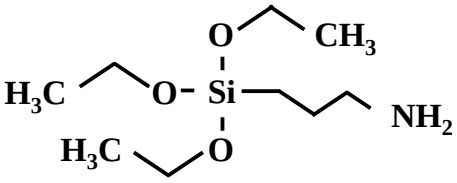

Figure 3. Molecular structure of (3-Aminopropyl)-triethoxysilane used in surface modification of AlN particles for effective thermal coupling with PVDF matrix.

2.2.2 Nanocomposite synthesis

To prepare AlN/xGNP-PVDF nanocomposites with various filler volume fractions, silane treated AlN particles and xGNP particles of required weight are first sonicated in acetone for 2 h to form a stable dispersion. The PVDF powder is mixed into a 1:3 acetone:N,N-Dimethylformamide (DMF) solution at 70°C using a magnetic stirrer. The acetone-nanoparticle dispersion is then added to the PVDF slurry and stirred for 10 min while maintaining the temperature at 70°C. Lastly, the composite is transferred into a glass dish, allowed to set in an oven at 70°C for 24 h and finally hot pressed at 12.5 MPa and 200°C. Samples with 350-500 μm thickness and 1cm x 1cm surface area are obtained using the above procedure.

2.3 Characterization of nanocomposites

The thermal conductivity of the nanocomposites is measured using a comparative technique extended from ASTM standard E1225, using infrared microscopy for temperature measurement [16]. In this method, the sample is sandwiched between two quartz layers (reference material with known thermal conductivity) and a one-dimensional heat flux is generated across the stack

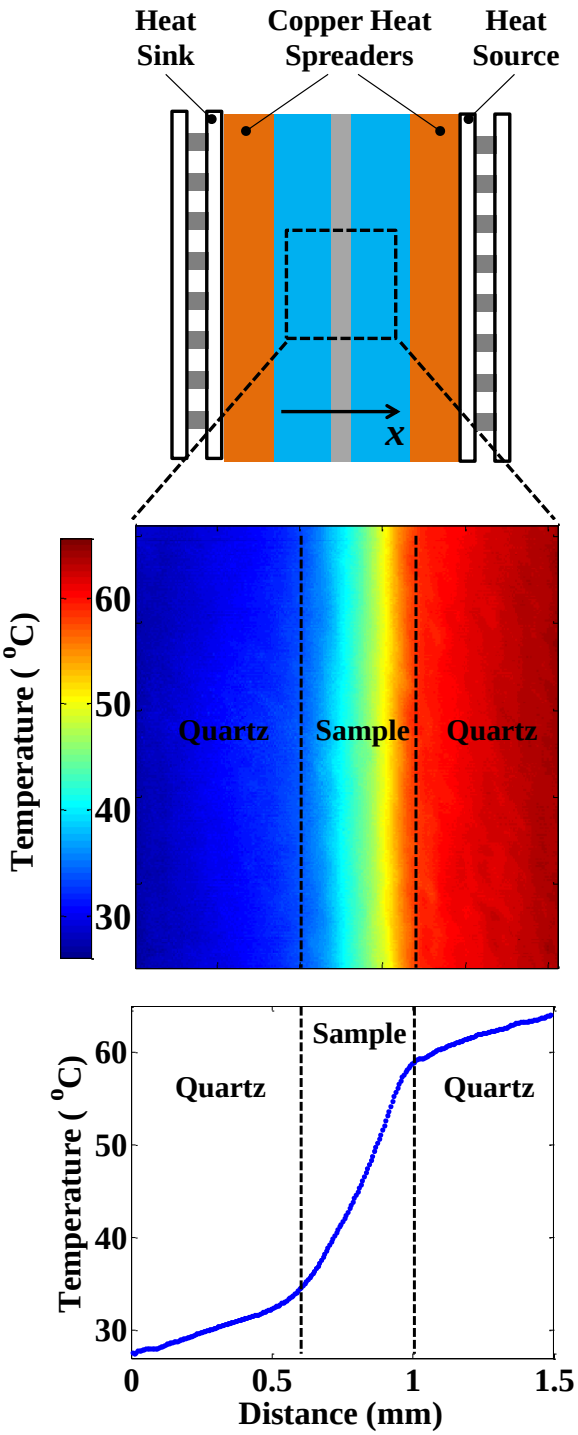

Figure 4: Infrared microscopy for thermal conductivity measurement of nanocomposites. Top: Schematic of experimental set up which establishes a one-dimensional heat flux across quartz/sample/quartz stack. The test sample is sandwiched between two reference quartz layers and subjected to heat flux in the negative x-direction using two thermoelectric modules. Copper heat spreaders are inserted between thermoelectric modules and quartz slides to ensure uniform temperature perpendicular to x-axis. Middle: Temperature map of quartz/PVDF/quartz stack obtained from IR microscope. Bottom: Temperature profile across the stack after averaged in direction normal to heat flux.

using thermoelectric modules as heat source and sink on either ends as shown in Figure 3(top). Copper heat spreaders placed between the quartz slides and thermoelectrics spread the heat and ensure one-dimension heat flow, *e.g.* the uniform temperatures in the planes perpendicular to heat transport. A thin layer of graphite paint on the top faces of quartz slides and composite samples provides nearly uniform, near unity emissivity, which is advantageous for the IR temperature mapping. This graphite-coated test surface is calibrated for emissivity before temperature measurements. An IR microscope (Quantum Focus Instruments) is used to obtain two-dimentional temperature maps with spatial resolution of ~5.9 μm and temperature resolution of 0.1^{o}C. An example temperature map is shown in Figure 3(middle). This temperature map is averaged in a direction perpendicular to heat flux to obtain the one-dimensional temperature profile across the stack, as shown in Figure 3 (bottom). The thermal conductivity of the composite sample is then obtained using Eqn. 1. The uncertainty in each measurement is calculated from the difference in temperature gradients in the hot and cold quartz layers (Eqn. 2).

$$\frac{k_{sam}}{k_{ref}} = \frac{\left(\frac{dT}{dx}\right)_{ref,cold} + \left(\frac{dT}{dx}\right)_{ref,hot}}{2\left(\frac{dT}{dx}\right)_{sam}} \quad .....(1)$$

$$\%\, err = 2\,\frac{\left|\left(\frac{dT}{dx}\right)_{ref,cold} - \left(\frac{dT}{dx}\right)_{ref,hot}\right|}{\left(\frac{dT}{dx}\right)_{ref,cold} + \left(\frac{dT}{dx}\right)_{ref,hot}} \text{x}\,100 \quad .....(2)$$

3 RESULTS AND DISCUSSION

The thermal conductivity of PVDF-xGNP composites increases approximately linearly with volume fraction as shown in Figure 5. For the sample with 5 vol% xGNP, the thermal conductivity increases by ~ 238% compared to the pure PVDF samples. The thermal conductivity of PVDF-AlN is shown in Figure 6a. Inorder to limit the electrical conductivity enhancement in the composites, the xGNP volume fractions are limited to 5% and much higher volume fractions of AlN particles are used. However, the thermal conductivity of PVDF-AlN composites increases less rapidly with volume fraction compared to the xGNP samples.

Figure 6a shows the thermal conductivity of composites with 2 vol% xGNP and varying concentrations of AlN nanoparticles and Figure 6b shows the thermal conductivity of composites with 40 vol% AlN and varying concentrations of xGNPs. Under the assumptions that filler particles do not interact with each other (that is, they do not form effective percolation networks) and there is no boundary resistance at the particle-matrix interface, Maxwell's equation (see Eqn 3) can predict the effective thermal conductivity of composites [17]. Considering the PVDF as the matrix material for the AlN composites and 2 vol% of xGNP composite as the matrix material for the AlN+2 vol% of xGNP composites, the thermal conductivity is evaluated using Maxwell's equation (see Figure 6a). In a similar manner, using each of the 1-5 vol% of xGNP as matrix materials, the effective thermal condutivities of 40 vol% AlN+ xGNP composites can be computed (see Figure 6b).

$$\frac{k_e - k_m}{k_e + 2k_m} = f_p\left(\frac{k_p - k_m}{k_p + 2k_m}\right) \quad .....(3)$$

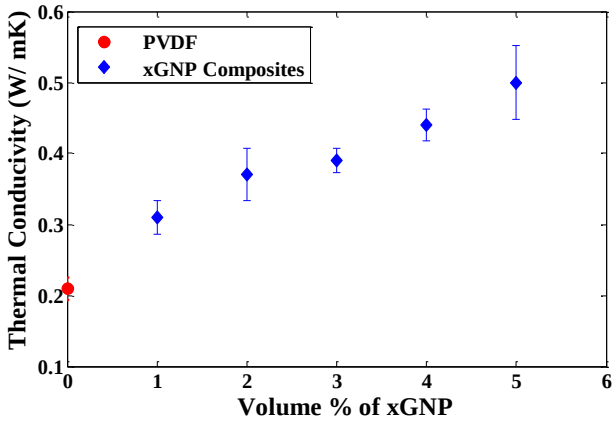

Figure 5: Thermal conductivity of PVDF-xGNP composites.

AlN particles have an aspect ratio near one and do not form effective thermal percolation networks at low filler vol%. For AlN composites with concentrations 40 vol% and below, the measured thermal conductivity matches well with that from Maxwell's equation, while the thermal conductivity of PVDF-50 vol% AlN composite is higher than the predicted value, which indicates that the percolation threshold is ~ 40 vol%. Addition of 2 vol% of xGNP to the AlN composites yielded moderate enhancement in thermal conductivity at low AlN volume fractions and significant enhancements for the samples with 40 and 50 vol% AlN, indicating an onset of effective percolation at 40 vol%. Composites with 50 vol% AlN and 2 vol% xGNP showed an order of magnitude improvement in thermal conductivity over PVDF.

Composites with 40 vol% AlN + 1-5 vol% xGNP showed a linear trend in thermal conductivity enhancement with increasing xGNP vol%. As shown in Figure 6b, effective percolation paths are established in the AlN-xGNP composites, even at low vol % of xGNP as indicated by comparsion with result from Maxwell's equation. At 1 vol% xGNP-40 vol% AlN, a thermal conductivity enhancement of ~ 2.7 is achieved compared to the PVDF-40 vol% AlN composite. In contrast, an

enhancement of ~1.4 is achieved for the 1 vol% xGNP composite (with no AlN) when compared to the PVDF matrix (see Figure 5). This is a clear indication of a synergic effect between AlN and xGNP particles.

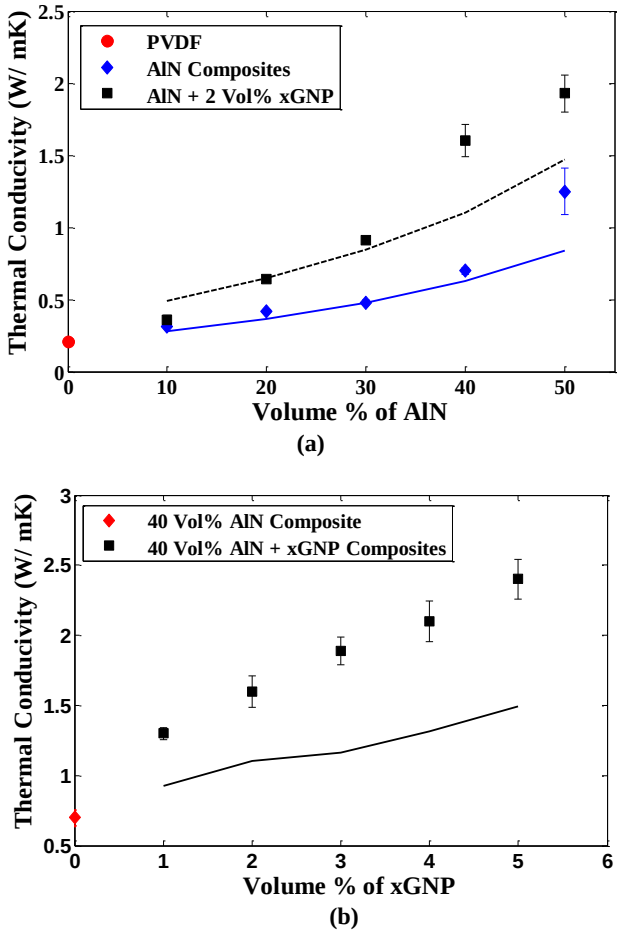

Figure 6: Thermal conductivity of PVDF-AlN-xGNP composites. a) Thermal conductivity of composites with varying concentrations of AlN nanoparticles in 2 vol% xGNP. Solid line and dashed line are effective thermal conductivities calculated from Maxwell's equation using PVDF and PVDF-2 vol% xGNP composite as matrix materials, respectively. b) Thermal conductivity of composites with 40 vol% AlN and varying concentrations of xGNPs. Solid line is the effective thermal conductivity calculated from Marwell's equation using each of the 1-5 vol% of xGNP as matrix materials.

4 CONCLUSIONS

The measured thermal conductivity of AlN and xGNP composites in PVDF is compared to predictions from effective medium theory based on Maxwell's equation. AlN composites show an onset of percolation for ~ 40 vol% AlN. Impact of adding 2 vol% xGNP to the AlN composites on their thermal conductivity also show evidence of strong percolation for AlN concentrations of 40 vol% and more. Comparion of thermal conductivity enhancement in 1 vol% xGNP over PVDF and 1 vol% xGNP + 40 vol% AlN over 40 vol% AlN indicate strong synergy between AlN and xGNP particles.

ACKNOWLEDGMENTS

The authors gratefully acknowledge the financial support of Semiconductor Research Corporation (SRC) through task 1996.01.

References:

[1] K.N. Tu, "Reliability challenges in 3D IC packaging technology," Microelectronics Reliability, vol. 51 (2011), 517–523

[2] Pulkit Jain, Pingqiang Zhou, Chris H. Kim, and Sachin S. Sapatnekar , "Three Dimensional Integrated Circuit Design Integrated Circuits and Systems," Springer Link (2010), 33-61

[3] Ankur Jain, Robert E. Jones, Ritwik Chatterjee, and Scott Pozder, "Analytical and Numerical Modeling of the Thermal Performance of Three-Dimensional Integrated Circuits," IEEE Transactions on Components and Packaging, vol. 33 (2010) 1, 56-63

[4] John Philip, P D Shima and Baldev Raj, "Evidence for enhanced thermal conduction through percolating structures in nanofluids," Nanotechnology, vol. 19 (2008), 305706 (7pp)

[5] Xuejiao Hu, Linan Jiang, and Kenneth E. Goodson, "Thermal Conductance Enhancement of Particle-filled Thermal Interface Materials Using Carbon Nanotube Inclusions," Proceedings of Inter Society Conference on Thermal Phenomena, vol.1 (2004), 63 - 69

[6] Chih-Chun Teng, Chen-Chi M. Ma, Kuo-Chan Chioub, Tzong-Ming Lee, Yeng-Fong Shih, "Synergetic effect of hybrid boron nitride and multi-walled carbon nanotubes on the thermal conductivity of epoxy composites," Materials Chemistry and Physics, vol. 126 (2011) 722–728

[7] K. C. Yung, H. Liem, "Enhanced Thermal Conductivity of Boron Nitride Epoxy-Matrix Composite Through Multi-Modal Particle Size Mixing," Journal of Applied Polymer Science, vol. 106 (2007), 3587–3591

[8] Yunsheng Xu, D. D. L. Chung, Cathleen Mroz, "Thermally conducting aluminum nitride polymer matrix composites," Composites: part A, vol. 32 (2001), 1749-1757

[9] Zhongqi Shi, Mohamed Radwan, Soshu Kirihara, Yoshinari Miyamoto and Zhihao Jin, "Enhanced thermal conductivity of polymer composites filled with three-dimensional brushlike AlN nanowhiskers," Applied physics letters, vol. 95 (2009), 224104

[10] Tianle Zhou, Xin Wang, G.U. Mingyuan, Xiaoheng Liu, "Study of the thermal conduction mechanism of nano-SiC/DGEBA/EMI-2,4 composites," Polymer, vol. 49 (2008) 4666–4672

[11] Woong Sun Lee, Jin Yu, "Comparative study of thermally conductive fillers in underfill for the electronic components," Diamond & Related Materials, 14 (2005) 1647 – 1653

[12] H. Fukushima, L. T. Drzal, B. P. Rook, and M. J. Rich, "Thermal Conductivity of Exfoliated Graphite Nanocomposites," Journal of Thermal Analysis and Calorimetry, vol. 85 (2006) 1, 235–238

[13] Aiping Yu, Palanisamy Ramesh, Mikhail E. Itkis, Elena Bekyarova, and Robert C. Haddon, "Graphite Nanoplatelet-Epoxy Composite Thermal Interface Materials," Journal of Physical Chemistry Letters C, vol.111 (2007), 7565-7569

[14] Y.C. Li, S.C. Tjong, and R.K.Y. Li, "Electrical conductivity and dielectric response of poly(vinylidenefluoride)–graphite nanoplatelet composites," Synthetic Metals, vol. 160 (2010), 1912–1919

[15] Yunsheng Xu, and D. D. L. Chung, "Increasing the thermal conductivity of boron nitride and aluminum nitride particle epoxy-matrix composites by particle surface treatments," Composite Interfaces, vol. 7(2000) 4, 243-256

[16] Marconnet, A.M., et al., "Thermal Conduction in Aligned Carbon Nanotube-Polymer Nanocomposites with High Packing Density," ACS Nano, vol. 5 (2011) 6, 4818-4825

[17] J. C. Maxwell, "Treaties on Electricity and Magnetism," Clarendon Press, Oxford, 1873